Volume 17, Number 5, 2024. pp. 639-646

Jordan Journal of Physics

ARTICLE

Enhanced Room Temperature Ammonia Gas Sensing Response of DC Magnetron Sputtered Vanadium Oxide Thin Films

A. Paramesvaran[a], **M. Balachandramohan**[b], **P. Sivakumar**[c] and **P. Devaraj**[c]

[a] *Department of Physics, Sri Vasavi College, Erode, Tamil Nadu 638316, India.*

[b] *Department of Physics, Erode Arts and Science College, Erode-, Tamil Nadu 638009, India.*

[c] *Department of Physics, Bharathiar University, Coimbatore, Tamil Nadu 641046, India.*

Doi: **https://doi.org/10.47011/17.5.11**

Received on: 03/07/2023; *Accepted on: 12/09/2023*

Abstract: In this study, the sensitive selective ammonia (NH_3) gas sensor was fabricated using V_2O_5 thin films synthesized by DC (direct current) magnetron sputtering technique with different substrate temperatures. The sputtered V_2O_5 thin films were analyzed for their optical, structural, morphological, and gas-sensing properties. X-ray diffraction (XRD) and Raman spectroscopy results indicated that the thin films were amorphous. The gas-sensing performance was evaluated at various substrate temperatures and different NH_3 concentrations ranging from 5 to 200 ppm, with 27 °C as the operating temperature. The V_2O_5 thin films achieved their maximum response to NH_3 at room temperature (27°) and an optimal ammonia concentration of 100 ppm. Notably, the room-temperature-sputtered V_2O_5 sensors showed a good gas-sensing response of 45.94%. After 50 days, the gas response to the same NH_3 concentration was nearly 44.23%. Furthermore, all sputtered gas sensors demonstrated good selectivity toward NH_3 over other gases, including acetone, methanol, ethanol, and toluene, as well as long-term stability.

Keywords: Sputtering, Gas sensing response, Operating temperature, Sensitivity, Selectivity.

1. Introduction

Detecting and monitoring toxic ammonia gas plays a major role in human health and safety. The scientific community has focused on gas sensors based on metal oxide semiconductors (MOS), such as V_2O_5, SnO_3, ZnO, and TiO_2. The properties of these semiconducting materials, particularly their response to target gases, can significantly enhance sensitivity when exposed to n-type or p-type materials commonly used in gas sensing applications. MOS sensors offer several advantages, including ease of fabrication at low cost, fast response times, high sensitivity, and good selectivity, which can be further improved by optimizing the morphology of the sensing material.

Vanadium oxide is a metal oxide semiconductor with good optical and electrical properties due to the multivalent state of electrons. For this reason, significant attention has been given to the development of gas sensors based on this material. Vanadium can exist in various valence states and exhibits Magneli phases such as VO_2, V_2O_3, V_6O_{13}, and V_2O_5. V_2O_5 thin films are used in various applications such as actuators, memory devices, optical switching devices, and electrochromic display devices [1–4]. One-dimensional structured V_2O_5 holds great promise for the development of gas sensors that operate at room temperature [5]. Due to its multivalent nature, the wide bandgap

Corresponding Author: A. Paramesvaran **Email**: yashvanthparamesvaran@gmail.com

of 2.3 eV, good thermal stability, and chemical properties, vanadium pentoxide (V_2O_5) is an excellent material for gas sensing [6, 7]. The sensing response of various types of gas sensors—such as semiconductor gas sensors [8–10], optical gas sensors [11–13], and solid electrolyte gas sensors [14]—depends on the type of sensing material used. Several preparation methods exist, including electron beam evaporation [15], DC magnetron sputtering [16], chemical vapor deposition [17], spray pyrolysis [18, 19], and spin coating [20]. Among these methods, we chose DC magnetron sputtering for thin film preparation due to its uniform deposition and top-down process.

In the initial step of our work, V_2O_5 thin films were fabricated by the DC magnetron sputtering technique at different substrate temperatures. In the next step, a characterization analysis was performed to assess the structural, morphological, and optical properties of the films. The final step involved evaluating the gas sensing performance of the films at various ammonia concentrations (5–200 ppm).

2. Experimental Procedure

2.1. Preparation of Thin V_2O_5 Film Ammonia Gas Sensors

V_2O_5 thin films were deposited onto well-cleaned Si glass substrates using a DC magnetron sputtering system (manufactured by Hind High Vacuum, India). A vanadium target with 99.995% purity, a diameter of 76.2 mm, and a thickness of 3.175 mm was used. Proper cleaning of the substrates was critical to obtaining high-quality thin films. The cleaning process involved immersing the substrates in a KOH solution, followed by rinsing with distilled water. Subsequently, the substrates underwent ultrasonic treatment in acetone and isopropanol for 10 minutes. Afterward, they were rinsed again with distilled water, acetone, and isopropanol to eliminate contaminants and surface irregularities.

The cleaned substrates were positioned at a distance of 80 mm from the target holder. The vacuum system, equipped with rotary and diffusion pumps, achieved a base pressure of 2.5×10^{-5} mbar. To remove contamination from the target, a pre-sputtering process was performed in a high-purity argon atmosphere. During sputtering, a cathode power of 60 watts was maintained, and the films were deposited at various substrate temperatures. The optimized growth parameters are summarized in Table 1.

TABLE 1. Optimized growth parameters of the V_2O_5 thin film.

Substrate Temperature °C	Sputtering Power(W)	Deposition time (min)	Base pressure mbar	O_2 pressure mbar	O_2 flow sccm	Sample code
RT	60	20	$2.5X10^{-5}$	$8.7X10^{-4}$	3	VOA1
100	60	20	$2.5X10^{-5}$	$8.7X10^{-4}$	3	VOA2

2.2. Materials and Characterization

The structural analysis was performed using an X-ray diffractometer model (Bruker D8Advance), which has a Cu Kα wavelength of 1.5406 Å with 2θ varying from 10 to 80°. The morphological study was done with the help of scanning electron micrographs (Quanta FEG 250). Raman spectrum analysis was carried out using an argon-ion laser (LabRAM HR, Horiba, France) with a wavelength range of 200–2100 nm. Elemental analysis was conducted with an energy-dispersive X-ray spectrometer (EDX) integrated into the Quanta FEG 250 system. Optical transmittance and the optical band gap were determined using a UV-visible spectrophotometer (Varian 5000) within a wavelength range of 300–3000 nm.

2.3. Sensor Fabrication and Measurement Setup

The fabricated ammonia sensors were deposited on the Ag-coated thin film, which acts as electrodes. The sensors were placed inside a custom-built gas sensing setup for ammonia detection. The sensor's response, based on resistance changes, was measured using a Keysight B2902A digital source meter.

During operation, the sensor was positioned at the center of the chamber, and a certain amount of ammonia gas was introduced, mixed with dry synthetic air, using a mass flow controller. The operating temperature, ranging from 27°C to 100°C, was adjusted using a temperature controller. In most metal oxide thin

films, resistance increases when ammonia gas enters the chamber.

A schematic representation of the gas sensing setup is shown in Fig. A.

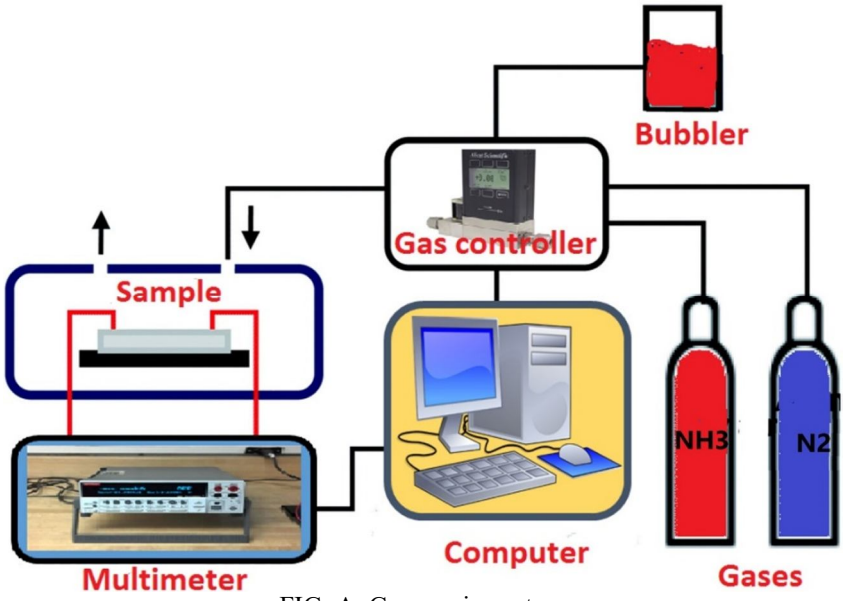

FIG. A. Gas sensing setup.

3. Results and Discussion

3.1. Optical Properties

The sensor's transmittance and band gap energy mainly depend on deposition parameters. The transmittance curves were plotted in the 200 to 3000 nm wavelength range. The transmittance percentage and E_g of the two samples, VOA1 and VOA2, are shown in Figs. 1(a) and 1(b). The optical transmittance of the sensors in the visible region was approximately 84%, but it decreased with increasing substrate deposition temperature. Interestingly, the transmittance curves for both VOA1 and VOA2 thin films converged at wavelengths below 500 nm.

The energy band gap of the samples was calculated. The VOA1 sensor was dominant compared to the VOA2 sensor. Figure 1(b) shows a curve of $(\alpha h\nu)^{1/2}$ versus hν for both samples. It is used to calculate the band gap of the sensor using a Tauc plot for indirectly allowed transitions of values of VOA1 and VOA2 sensors, where E_g = 2.41 eV and Eg = 2.37 eV, respectively. These findings are consistent with the reported band gap energy range for pure V_2O_5 thin films (E_g = 2.12–2.47 eV) in the literature [21]. The estimated optical energy band gap of V_2O_5 thin films sputtered at various deposition temperatures is shown in Fig. 1(b). The optical band gap of the VOA2 sensor decreased with increasing substrate temperature, from 2.41 eV to 2.37 eV due to nano-level particle size.

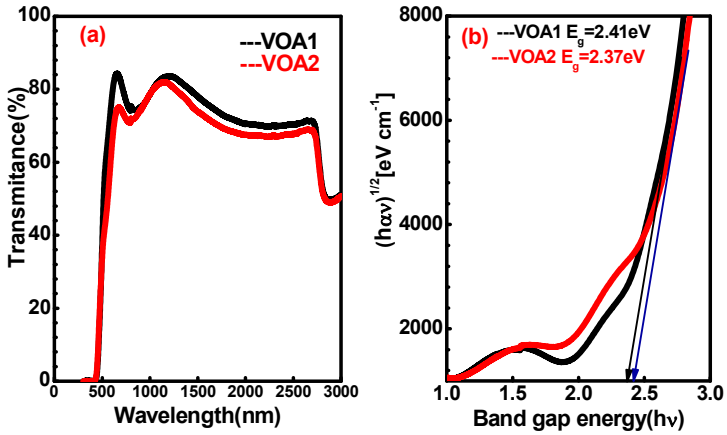

FIG. 1. (a) optical transmittance and (b) band gap energy of the V2O5 thin film.

3.2. Structural Analysis

The structural properties of the sputtered V2O5 sensors were analyzed using X-ray diffraction (XRD) spectra collected over a range of 10° to 80°, focusing on the effects of substrate temperature. The XRD patterns of the VOA1 and VOA2 sensors, shown in Figs. 2(a) and 2(b), indicate that the films are amorphous. This amorphous nature is advantageous for gas sensing applications, as it often results in higher selectivity and enhanced performance.

The diffraction angles observed at 20.54°, 27.57°, and 42.17° correspond to the (001), (110), and (002) planes, respectively, and align with the standard JCPDS data (JCPDS Card No. 00-041-1426). As previously reported, increasing the substrate temperature leads to sharper and more intense XRD peaks, which reflects an improvement in the crystallinity of the sensor, as seen in VOA2 [22–24].

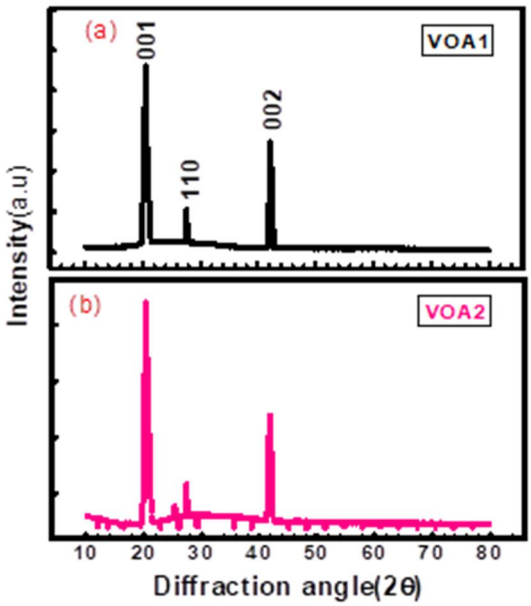

FIG. 2. XRD pattern of the V_2O_5 thin film.

3.3. Raman Studies

The Raman spectra of the VOA1 and VOA2 samples, fabricated as ammonia gas sensors via DC magnetron sputtering, were measured in the range of 80–1000 cm^{-1}, as shown in Fig. 3a and Fig. 3b. The observed Raman peaks correspond to the optical phonon vibrations of the V_2O_5 thin films. The symmetric and anti-symmetric stretching of the V-O bonds resulted in two prominent peaks with varying spectral intensities.

Our study indicates that optical phonons are the major source of electron scattering in the samples. Raman spectroscopy was employed to further investigate the optical characteristics of the V_2O_5 thin film sensors. Both XRD and Raman analyses confirm the strong amorphous nature of the samples. According to the Raman measurements, the layer consists exclusively of the pure V_2O_5 phase, which exhibits a predominantly amorphous and randomly oriented structure. The most prominent reflection is associated with the (110) orientation.

However, in the Raman spectra of the sputtered V_2O_5 thin films the peaks were more intense and better resolved in the films sputtered with an argon flow, while they became broader in the films deposited with added oxygen flow. It was obtained in the process and shows several sharp intense maxima located at 144 cm^{-1} and 410 cm^{-1}. The Raman spectrum of the film obtained in the process presents only a low intensity. The Raman spectrum of the films is obtained in the richest atmosphere of O_2. The major vibrational region in the Raman spectra for the vibrational oxide system is situated in the range of 80-1000cm^{-1}, with the V-O terminal stretching prominently occurring at 707 cm^{-1}. The Raman analysis highlights the influence of oxygen flow during the deposition process on the structural properties of the V_2O_5 films. The broad and weak Raman bands corresponding to films indicate the presence of a significant amorphous phase.

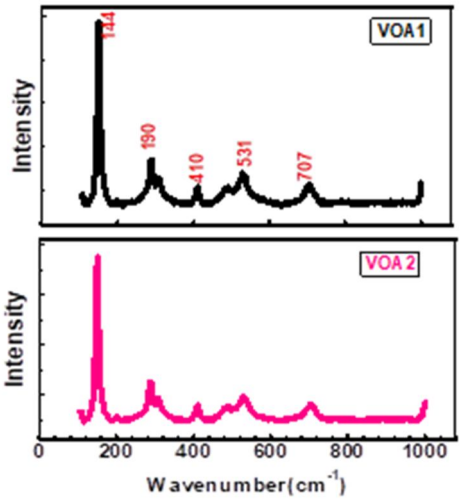

FIG. 3. The Raman spectrum of the VOA1 and VOA2 sensors.

3.4. Energy Dispersive X-Ray (EDX) SEM Analysis

EDX studies were used to find the elemental composition of the V_2O_5 thin films. Figures 4(a)

and 4(c) show that vanadium and oxygen are majorly present in V_2O_5 thin films. Additionally, trace elements such as Na, Ca, and Mg were detected in both VOA1 and VOA2 sensors. The elemental composition (in atomic percentage) for the VOA1 and VOA2 sensors was as follows: V (28.3, 28.8), O (32.1, 33.9), Na (25.7, 26.0), Mg (5.0, 5.0), and Ca (6.0, 5.0), respectively. Sensor elements V and O correspond to the V_2O_5 sputtered thin films. Figures 4(b) and 4(d) illustrate the SEM analysis, which reveals the surface morphology of the sensors. Both the VOA1 and VOA2 sensors exhibit a small flower-like morphology. This morphology is characterized by high porosity, making it highly suitable for gas sensing applications. The surface morphologies are compact and continuous, with closely packed particles. This compactness ensures that the electron mobility between grains is not significantly hindered. Large agglomerated grains were homogeneously distributed with good adhesion to the substrates. The EDX spectra elucidate that the synthesized composite thin films exhibit the presence of V and O only. No other remarkable impurities were observed.

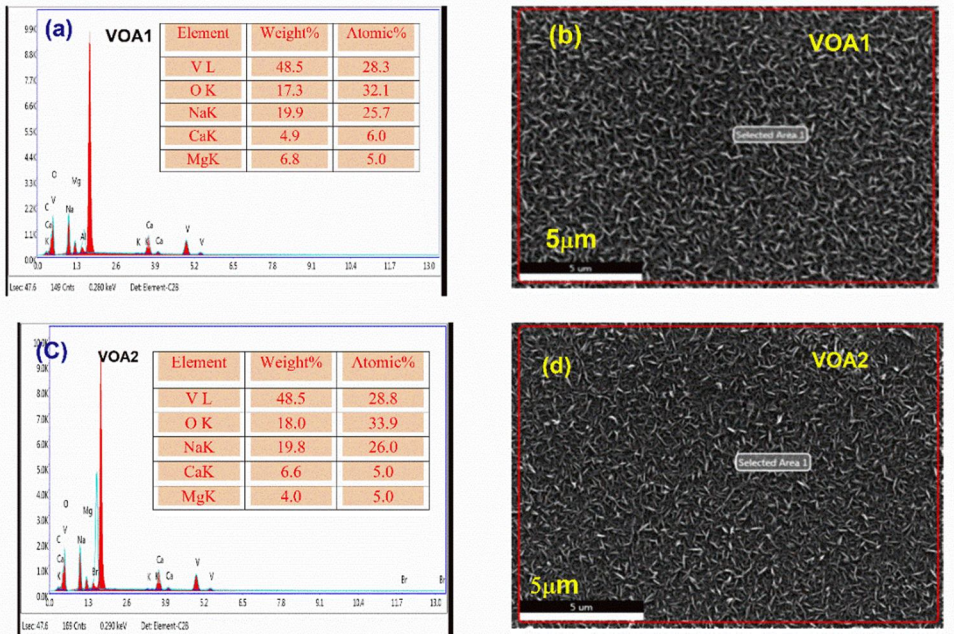

FIG. 4. (a) and (c) EDX -Compositional analysis of the V_2O_5 thin films, (b) and (d) SEM image of the V_2O_5 thin film.

3.5. Ammonia Sensing Studies

The electrical resistance changes due to gas responses to DC magnetron sputtering sensors were tested for several gases, mainly focusing on ammonia. Gas sensing measurements were conducted with the target gas and synthetic air. In metal oxide thin films, the resistivity typically increases when ammonia gas is allowed into the chamber. This behavior occurs due to sensor n-type semiconducting material as a result of electrons bonded with the adsorbed oxygen and transferred to thin films [25].

In general, the gas sensing response of the sensors is influenced by several factors, including the adsorption efficiency of ammonia gas molecules on the sensor surface, interactions between ammonia and adsorbed oxygen, surface morphology, crystalline size, and surface states [26]. Thin films with porous morphologies and large specific surface areas have been shown to exhibit high sensitivity and good reversibility, making them highly suitable for gas-sensing applications. Operating temperature is one of the most important parameters of gas sensing since it controls the adsorption and desorption processes. Initially, we examined the V_2O_5 sensor sensitivity at 100 ppm ammonia concentration at operating temperatures of 27 °C and 100 °C. As the operating temperature increased, the gas response decreased significantly. At 200 °C, no measurable gas response was observed. The operating temperature of 27° C was selected for all further measurements with different concentrations of ammonia for both sensors. Figures 5(a) and 5(b) show the change in resistance of the sensors at different concentrations of ammonia (5, 10, 50, 100, and 200 ppm) at 27° C as an operating temperature. For both sensors, the electrical resistance

increased with the increasing ammonia concentration. This behavior is attributed to the interaction of target gas molecules with adsorbed oxygen on the sensor surface, which results in the release of free electrons.

The released electrons recombine with holes in the semiconducting sensors, reducing the number of free charge carriers (holes and electrons) due to the recombination process. As a result, the resistance of the sensors increases.

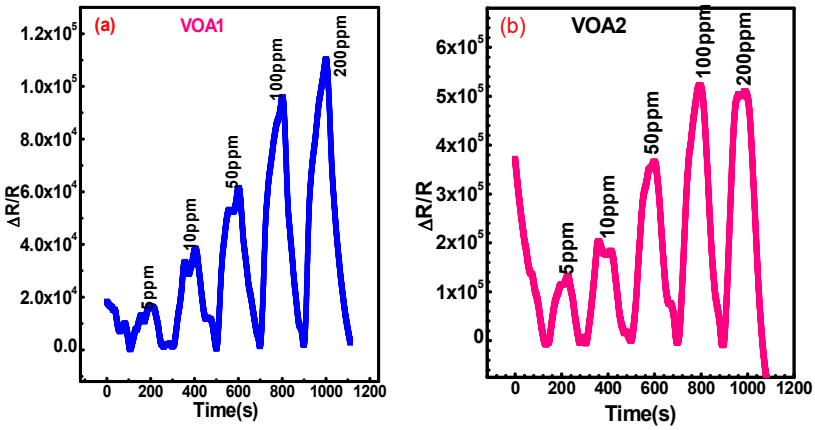

FIG. 5. Ammonia sensing response of the V2O5 thin film with different concentrations of 5-200ppm. (a) VOA1 (b) VOA2.

Figures 5(a) and 5(b) show the ammonia gas response of the sensors to different concentrations of ammonia. The gas-sensing response largely depends on the optimization conditions during the deposition process, which affect the surface morphology. The best gas response was observed one day after sensor fabrication. The VOA1 sensor exhibited a response of 12.59% at 5 ppm and 61.26% at 200 ppm, respectively. This enhanced response is attributed to the good surface roughness, which increases the number of adsorption sites available for interaction with the target gas.

In contrast, the VOA2 sensor showed a lower gas-sensing response due to its lower surface roughness, which resulted in fewer adsorption sites for ammonia molecules. The response for VOA2 ranged from 12.37% at 5 ppm to 30.61% at 200 ppm, reflecting a less efficient interaction with ammonia. This decreased performance can also be linked to the smaller crystalline size and less stable surface of the VOA2 sensor.

After 50 days, the gas-sensing response of both sensors was measured again at different ammonia concentrations. The VOA1 sensor showed almost no change in its gas-sensing response, maintaining similar values to those observed on day one. However, the VOA2 sensor's response decreased significantly, dropping to nearly half of the original values, indicating a loss of stability over time.

TABLE 2. Comparative sensitivity measurements with different concentrations of ammonia on day one and day 50.

Ammonia concentrations (ppm)	Gas response (%) After one day		Gas response (%) After 50 days	
	VOA1	VOA2	VOA1	VOA2
5	12.59	12.37	10.24	8.23
10	22.14	17.59	21.02	12.12
50	30.98	24.46	31.51	18.21
100	45.94	32.86	44.23	24.25
200	61.26	30.61	60.02	21.22

3.6. Stability, Reproducibility, and Selectivity

As shown in Figs. 6(a) and 6(b), the gas sensing response to NH_3 increases with the concentration of ammonia from 5 to 200 ppm for both the VOA1 and VOA2 sensors. Stability and reproducibility are essential for gas sensing applications. After 50 days, the films were examined under standard environmental laboratory conditions. The VOA1 sensor exhibited excellent reproducibility, maintaining a consistent response to 100 ppm ammonia, with similar results on both day one and day fifty. This indicates that the film's properties remained

unaffected by aging. In contrast, the gas sensing response of the VOA2 sensor decreased significantly over time. From this analysis, we conclude that the VOA1 sensor demonstrates better stability and long-term reliability compared to the VOA2 sensor at various ammonia concentrations.

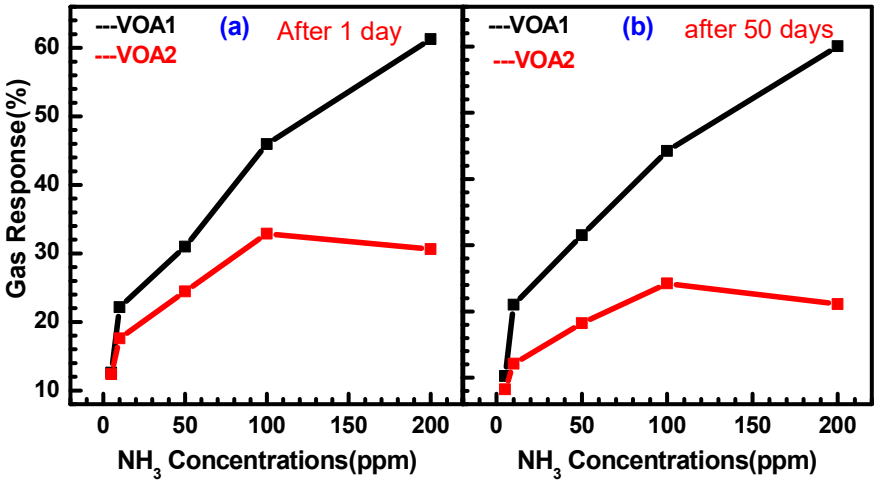

FIG. 6. Gas sensing response of VOA1 and VOA2 sensors with different concentrations of ammonia: (a) after one day and (b) after 50 days.

The selectivity of both sensors to detect a particular gas was evaluated. In this study, only four gases (ammonia, acetone, ethanol, and toluene) were detected using the DC magnetron sputtered V2O5 thin film sensor. The comparative histogram for the selectivity of VOA1 and VOA2 sensors at 100 ppm of each gas is shown in Figure 7. It was observed that both the VOA1 and VOA2 sensors demonstrated good sensing behavior towards ammonia. However, the VOA1 sensor showed greater stability when exposed to all the target gases.

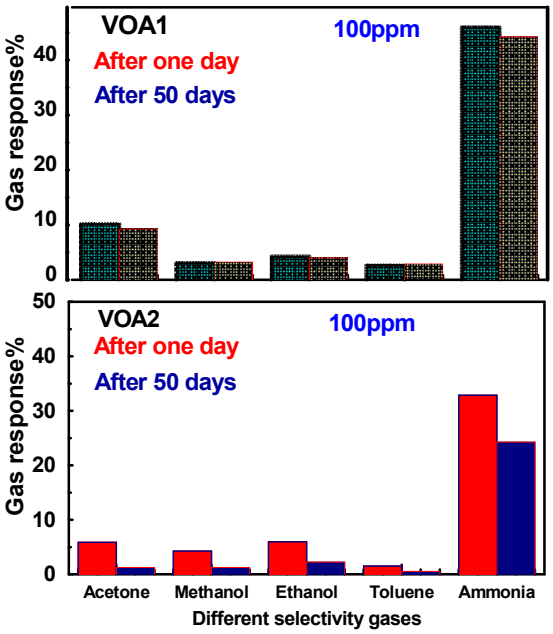

FIG. 7. Selectivity graph of VOA1 and VOA2 sensors for 100 ppm of different target gases.

Conclusion

V_2O_5 thin films were prepared using the cost-effective DC Magnetron sputtering. The structural, morphological, optical, and gas-sensing behaviors of the films varied with changes in substrate temperature. The band gap energy of the sensor decreased as the substrate temperature increased. The gas-sensing selectivity of the V_2O_5 sensor was studied for acetone, methanol, ethanol, benzene, and toluene at a concentration of 100 ppm. After 50 days, the gas-sensing response to ammonia showed a stable performance with outstanding sensitivity and selectivity towards various gases.

Acknowledgments

The authors are thankful to Dr. J.L. Jeyachandran, Department of Physics, Bharathiar University, for providing facilities for sensor fabrication. The authors would like to express their sincere gratitude to Dr. E.S. Kannan, Department of Physics, Birla Institute of Technology, Goa Campus, for supporting the characterization study.

Author contributions

Investigation, writing, and original draft preparation were done by A. Parameswaran and M. Balachandramohan. All authors have read and agreed to the published version of the manuscript.

Funding

This research work was done without any external funding.

Conflict of interest

There are no conflicts to declare.

References

[1] Fieldhous, N., Pursel, S.M., Horn, M.W., and Bharadwaja, S.S.N., J. Phys. D Appl. Phys., 42 (2009) 055408.

[2] Chen, K.H., Liao, C.H., Tsai, J.H., and Wu, S., Appl. Phys. A, 110 (2013) 211.

[3] Babeva, T., Awala, H., Grand, J., Lazarova, K., Vasileva, M., and Mintova, S., J. Phys. Conf. Ser., 992 (2018) 012038.

[4] Abbas, T.A., J. Electron. Mater., 47 (2018) 7331.

[5] Wang, R., Yang, S., Deng, R., Chen, W., Liu, Y., Zhang, H., and Zakharova, G.S., RSC Adv., 5 (2015) 41050.

[6] Boshta, M., Mahmoud, F.A., and Sayed, M.H., J. Ovonic Res., 6 (2010) 93.

[7] Schneider, K., Lubecka, M., and Czapla, A., Sens. Actuators B, 236 (2016) 970.

[8] Dey, A., Matter. Sci. Eng. B, 229 (2018) 206.

[9] Li, Z., Liu, X., Zhou, M., Zhang, S., Cao, S., Lei, G., Lou, C., and Zhang, J., J. Hazard. Mater., 415 (2021) 125757.

[10] Yamazoe, N., Sakai, G., and Shimano, K., Catal. Surv. Asia, 7 (2003) 63.

[11] Poongodi, S. et al., J. Alloys Compd., 719 (2007) 71.

[12] Nam, H.J., Sasaki, T., and Koshizaki, N., J. Phys. Chem. B, 110 (2006) 23081.

[13] Zheng, W. et al., Sens. Actuators B Chem. 329, 2020 129127.

[14] Espid, E. and Taghipour, F., Crit. Rev. Solid State Mater. Sci., 42 (5) (2017) 416.

[15] Ramana, C.V., Hussain, O.M., Naidu, B.S., and Reddy, P.J., Vacuum, 48 (1997) 431.

[16] Luo, Z, Wu, Z, Xu, X, Du, M, Wang, T, and Jiang, Y., Vacuum, 85 (2010) 145.

[17] Sahana, M.B. and Shivashankar, S.A., J. Mater. Res., 19 (2004) 2859.

[18] Akl, A.A., J. Phys. Chem. Solids, 71 (2010) 223.

[19] Irani, R., Rozati, S.M., and Beke, S., Mater. Chem. Phys., 139 (2-3) (2013) 489.

[20] Sahana, M.B., Sudakar, C., Thapa, C., Lawes, G., Naik, V.M., Baird, R.J., Auner, G.W., Naik, R., and Padmanabhan, K.R., Mater. Sci. Eng. B, 143 (1-3) (2007) 42.

[21] Ramana, C.V., Smith, R.J, Hussain, O.M., Chusueri, C.C., and Julien, C.M., Chem. Mater., 17 (2005) 1213.

[22] Vijayakumar, Y., Mani, G.K., Ramana Reddy, M.V., and Rayappan, J.B.B., Ceram. Int., 41 (2) (2015) 2221.

[23] Santos, R., Loureiro, J., Nogueira, A., Elangovan, E., Pinto, J.V., Veiga, J.P., Busani, T., Fortunato, E., Martins, R., and Ferreira, I., Appl. Surf. Sci., 282 (2013) 590.

[24] Kumar, A., Singh, P., Kulkarni, N., and Kaur, D., Thin Solid Films, 516 (2008) 912.

[25] Modafferi, V., Panzera, G., Donato, A., Antonucci, P.L., Cannilla, C., Donato, N., Spadaro, D., and Neri, G., Sens Actuators B, 163 (2012) 61.

[26] Rout, C.S., Hegde, M., and Govindaraj, A., Nanotechnology, 18 (2007) 20.